*Int. J. Heat Mass Transfer.* Vol. 32, No. 2, pp. 227–242, 1989
Printed in Great Britain

0017-9310/89 \$3.00+0.00
Pergamon Press plc

# Vapour bubble growth in boiling under quasi-stationary heat transfer conditions in a heating wall

M. V. FYODOROV
Department of Cryogenics, Moscow Power Engineering Institute, 105835 Moscow, U.S.S.R.

and

V. V. KLIMENKO
Department of Mechanical Engineering, Helsinki University of Technology, SF-02150 Espoo, Finland

(*Received* 1 *February* 1987)

**Abstract**—Consideration is given to the growth of vapour bubbles in boiling on a solid wall with small angles of wetting. It is shown that heat transfer in the wall under the bubble can occur in a quasi-stationary mode. The limits of the applicability of this approach are determined. The solution is given to the Laplace equation $\nabla^2 T = 0$ which describes the temperature field for the case considered. A theoretical relationship for the vapour bubble growth modulus with no empirical constants is obtained. The relationship quite satisfactorily predicts experimental data for cryogens, freons and other liquids that can easily wet a heating surface. It has been established that the effect of the heating surface material can be accounted for with the help of a simple parameter—the relative thermal conductivity $\lambda_w/\lambda_l$.

## 1. INTRODUCTION

THE PROBLEM of the growth of vapour bubbles in boiling has been the concern of a great number of theoretical and experimental investigations due, first of all, to the fact that the bubble growth rate enters, directly or indirectly, into the overwhelming majority of theoretical relations that describe the boiling heat transfer rate.

However, an accurate theoretical solution has been obtained only for the growth rate of a bubble in the bulk of a uniformly superheated liquid [1]. This is a well-known solution which agrees nicely with experimental data in a wide range of *Ja* [2, 3]. Attempts have been made to apply this solution to the bubble growth on a heating wall too. We shall not dwell in detail on those attempts here because the inadequacy of this approach has been rather conclusively demonstrated, e.g. in ref. [4]. Moreover, there exist a number of experimental investigations indicating that both the bubble growth rate and the heat transfer coefficient in boiling depend substantially on the thermal properties of the heating surface [2, 5–9].

Labuntsov [10] was the first to propose a relationship accounting for direct heat transfer from the heating wall to the bubble. It was assumed that the only thermal resistance on the way of the heat flux into the bubble was a liquid microlayer in the bubble base (Fig. 1). Then this heat flux can be very easily calculated as

$$q = \frac{\lambda_l}{\delta}(T_w - T_s). \tag{1}$$

It was assumed in this case that $T_w = \text{const.}$ As a result, the following theoretical relationship was obtained:

$$m = \frac{r_b}{\sqrt{(a_l\tau)}} = \sqrt{(\text{const.}\, Ja)} \tag{2}$$

where const. $\approx 12$. Equation (2) appears to be only a limiting case of a more complex relationship which takes into account the heat conduction in the heating wall itself. In fact, the assumption that $T_w$ is constant under a growing bubble can be realized only at high thermal conductivities of the wall, $\lambda_w$, whereas at low $\lambda_w$ the bubble will cool the adjacent parts of the wall.

Attempts to take into account the heat transfer in the wall itself were made [2, 7, 11], but in our opinion, all of them share one disadvantage, in all of these studies the authors used the solution of a one-dimensional problem of cooling a semi-infinite solid with these or other boundary conditions. It is well known, however, that the system geometry can be of fundamental importance in heat conduction problems. Thus, a spherical heat source immersed in an infinite body generates a heat flux in a quasi-stationary regime, whereas cylindrical and flat sources are unable to do this [12].

A specific feature of this paper is that it considers a three-dimensional temperature field rather than a one-dimensional one. It turns out that the heat transfer process in the heating wall under the bubble base often proceeds in a quasi-stationary regime thus signifying that it can be described by a stationary heat conduction equation.

## 2. STATEMENT OF A HEAT TRANSFER PROBLEM IN A HEATING WALL

An important parameter which influences the shape of the interface in three-phase systems is the wetting angle $\beta$. In a general case, the magnitude of this angle depends on many factors. This entails certain difficulties when constructing the bubble growth model in boiling. However, for a number of fluids the value of

## NOMENCLATURE

- $a$ radius in cylindrical coordinate system; thermal diffusivity
- $A$ dimensionless radius, $a/r_b$
- $c$ specific isobar heat capacity
- $Fo$ Fourier number, $a_w\tau_0/r_0^2$
- $h$ latent heat of vaporization
- $Ja$ Jakob number, $c_l\rho_l(T_w-T_s)/h\rho_v$
- $m$ dimensionless bubble growth modulus, $r_b/\sqrt{(a_l\tau)}$
- $q$ specific heat flux
- $q_l$ value of $q$ in the microlayer under the bubble base, $-\lambda_l((T_w-T_s)/\delta)$
- $q_v$ heat produced per unit volume
- $q_w$ value of $q$ in the wall on the boundary with liquid, $-\lambda_w(\partial T/\partial z)|_{z=0}$
- $Q$ heat flow rate
- $\hat{Q}$ dimensionless value of $Q$, $Q/(r_b\lambda_l\theta_s)$
- $Q_l$ heat flow rate entering the bubble from the surrounding superheated liquid
- $Q_w$ heat flow rate transferred from the wall
- $r$ radius in spherical coordinate system
- $r_b$ radius of a spherical bubble
- $r_0$ bubble departure radius
- $R$ dimensionless radius, $r/r_b$
- $T$ temperature
- $T_\infty$ temperature at infinite distance from the coordinate origin
- $T_s$ saturation temperature
- $T_w$ wall temperature at the boundary with liquid
- $U$ radial liquid velocity in the spherical coordinate system the origin of which coincides with the bubble centre
- $U_b$ value of $U$ on the vapour–liquid interface
- $V_b$ bubble volume
- $z$ coordinate
- $Z$ dimensionless coordinate, $z/r_b$

Greek symbols

- $\alpha$ angle in cylindrical and spherical coordinate systems
- $\beta$ angle of wetting (contact angle)
- $\gamma$ parameter found from formula (80)
- $\delta$ microlayer thickness
- $\delta_T$ thickness of superheated liquid layer formed on the wall in nucleate boiling
- $\Delta$ dimensionless thickness of microlayer, $\delta/r_b$
- $\theta$ temperature drop, $T-T_\infty$
- $\theta_s$ total temperature drop, $T_s-T_\infty$
- $\Theta$ dimensionless temperature drop, $\theta/\theta_s$
- $\Theta_0$ value of $\Theta$ on the boundary between regions I and II (Fig. 8)
- $\lambda$ thermal conductivity
- $\xi$ relative thermal conductivity, $\lambda_w/\lambda_l$
- $\rho$ density
- $\tau$ time from bubble initiation
- $\tau_0$ time of bubble growth prior to departure
- $\phi$ angle in spherical coordinate system.

Subscripts

- l liquid
- v vapour
- w wall
- ^ dimensionless quantity.

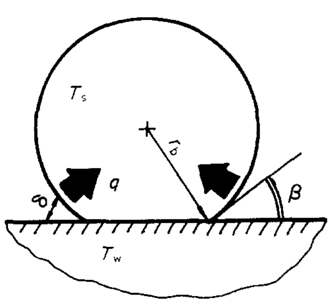


FIG. 1. Scheme of vapour bubble growth according to ref. [10].

$\beta$ is sufficiently stable. This refers, first of all, to cryogens for which $\beta$ varies in the range 0°–15° [2]. Freons [13] also have low wetting angles. Rather low values of $\beta$ (10°–25°) are typical of some organic fluids, such as ethanol, benzene, and propanol [14]. We shall confine our attention only to these groups of fluids that can easily wet heating surfaces, thus allowing the influences of $\beta$ to be disregarded and to assume for certainty that

$$\beta = 0^\circ. \tag{3}$$

We will assume further that the vapour–liquid interface has a spherical shape. According to experimental evidence, this assumption holds true at small $Ja$, whereas at high $Ja$ the shape of the surface becomes slightly distorted and this can influence the bubble growth rate. The latter can narrow the $Ja$-based range of validity of the results obtained. Specific recommendations regarding the above will be given in Section 6 on the basis of the comparison between theoretical and experimental values of the growth module at different $Ja$.

The latter assumption, with relation (3) taken into account, implies that the bubble has the shape of a sphere which touches the wall at one point (in what follows the zone of bubble contact with the wall will be discussed at some length).

We shall consider the problem in the spherical $(r, \phi, \alpha)$ and cylindrical $(a, z, \alpha)$ coordinate systems as shown in Fig. 2. It will be assumed in the cases that follow that the temperature field is independent of

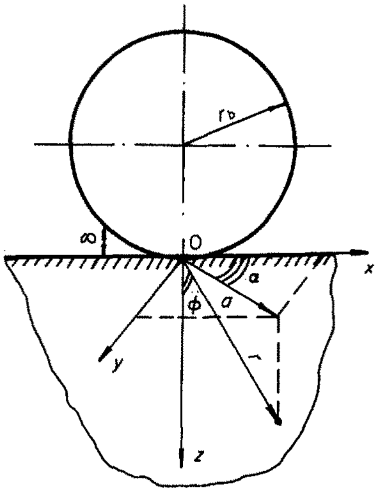


FIG. 2. Proposed model of the vapour bubble.

angle $\alpha$, therefore from now on this coordinate will not be indicated.

The thickness of the liquid layer under the downward facing spherical bubble surface can be found from

$$\delta = r_b - \sqrt{(r_b^2 - a^2)}. \tag{4}$$

This layer will be traditionally referred to as a 'microlayer' even though in our formulation its maximum thickness amounts to $r_b$ at $a = r_b$. The specific heat flux transferred from the wall to the bubble through this microlayer will be calculated from equation (1), using equation (4), but bearing in mind that the wall surface temperature $T_w$ in our problem may depend on the coordinate $a$ and time $\tau$. We will also assume that when $a > r_b$, there is no heat transfer on the boundary of the solid wall.

In remote zones ($a \to \infty$ or $z \to \infty$) the wall temperature is independent of space and time and is equal to $T_\infty$.

We will further assume that the liquid and wall material properties are constant in the temperature range $T_s$–$T_\infty$.

The heat exchange between the bubble and the surrounding liquid (except the 'microlayer') will be neglected now. Its influence will be considered later, in Section 5.

The above assumptions allow one to formulate the following system of boundary conditions for the heat conduction process in the wall (in the cylindrical system of coordinates):

$$z = 0, \quad a \leqslant r_b, \quad \lambda_w \frac{\partial T}{\partial z} = \frac{\lambda_l}{\delta}(T_w - T_s) \tag{5}$$

$$z = 0, \quad a > r_b, \quad \lambda_w \frac{\partial T}{\partial z} = 0 \tag{6}$$

$$z \to \infty \text{ or } a \to \infty, \quad T \to T_\infty. \tag{7}$$

In order to calculate heat transfer to the bubble from the heating wall, it is necessary to solve the equation of heat conduction in the wall (with the above boundary and some initial conditions):

$$\frac{\partial T}{\partial \tau} = a_w \nabla^2 T + \frac{q_v}{c_w \rho_w}. \tag{8}$$

We shall assume that all the heat is transferred to the bubble from the peripheral zones of the wall, i.e. the power of the inner heat sources is equal to zero. Then equation (8) will be reduced to

$$\frac{\partial T}{\partial \tau} = a_w \nabla^2 T. \tag{9}$$

Under certain conditions this equation can be considerably simplified. Indeed, in the case of slow bubble growth and high values of $a_w$ it is possible to ignore the term $\partial T/\partial \tau$ in equation (9) and the latter will go over into the Laplace equation

$$0 = \nabla^2 T. \tag{10}$$

This means that for each value of $r_b$ there will develop in the wall a steady state which will correspond to boundary conditions (5)–(7). It is therefore natural that the heat flux transferred to the bubble under these conditions will depend on $r_b$ and consequently on $\tau$. In other words, in this case the non-stationary heat transfer is realized in such a way that the system at hand passes successively through an infinite number of stationary states. In this sense the heat transfer in the wall can be called quasi-stationary.

## 3. STATIONARY SOLUTION

Consider the solution of the said problem for the case of quasi-stationary heat conduction in a wall (in the cylindrical system of coordinates). Under the assumptions made heat transfer is completely determined by the following set of variables: $r_b$, $\lambda_l$, $\lambda_w$, $\theta_s$, $a$, $z$. Obviously, it is possible to write for the temperature difference and heat flux from the wall to the bubble that

$$\theta = f_1(r_b, \lambda_l, \lambda_w, \theta_s, a, z) \tag{11}$$

$$Q_w = f_2(r_b, \lambda_l, \lambda_w, \theta_s). \tag{12}$$

Further, using dimensional analysis we can obtain, respectively, that

$$\Theta = \hat{f}_1(\xi, A, Z) \tag{13}$$

$$\hat{Q}_w = \hat{f}_2(\xi). \tag{14}$$

It is the search for relations (13) and (14) that the present section will deal with.

The dimensionless specific heat fluxes at the wall–liquid boundary can be expressed as

$$\hat{q}_l = q_l \frac{r_b}{\lambda_l \theta_s} \tag{15}$$

$$\hat{q}_w = q_w \frac{r_b}{\lambda_l \theta_s}. \tag{16}$$

Equation (10) with boundary conditions (5)–(7) can be nondimensionalized as follows:

$$\nabla^2\Theta = 0 \tag{17}$$

$$Z = 0, \quad A \leqslant 1, \quad \hat{q}_w = \hat{q}_l \tag{18}$$

where

$$\hat{q}_l = (1-\Theta)/\Delta \tag{19}$$

$$Z = 0, \quad A > 1, \quad \hat{q}_w = 0 \tag{20}$$

$$A \to \infty, \quad \Theta \to 0 \tag{21}$$

$$Z \to \infty, \quad \Theta \to 0. \tag{22}$$

We have solved equation (17), with boundary conditions (18)–(22), by numerical methods on the basis of Thomas' exact solution [15] for a semi-infinite solid body which receives heat flux uniformly distributed over the area of some circle of radius $b$ (Fig. 3).

Thomas had obtained the following expressions for the surface temperature of the body ($z = 0$):

when $0 < a < b$

$$\theta = \frac{2}{\pi}\frac{q_w b}{\lambda_w}E\left(\frac{a}{b}\right); \tag{23}$$

when $a > b$

$$\theta = \frac{2}{\pi}\frac{q_w a}{\lambda_w}\left[E\left(\frac{b}{a}\right) - \left(1-\frac{b}{a}\right)^2 K\left(\frac{b}{a}\right)\right] \tag{24}$$

where $K$ and $E$ are complete elliptical integrals of the first and second kind, respectively. Using the superposition method, it is not difficult to obtain, from the above solution, the temperature distribution for the case of an annular heat source with the outer and inner radii $b_{i+1}$ and $b_i$, respectively. To this end, it suffices to subtract the solution for the circle of radius $b_i$ from the solution for the circle of radius $b_{i+1}$. For instance, for the case of $0 < a < b_i < b_{i+1}$ we can obtain (using equation (23)) that

$$\theta_i = \frac{2}{\pi}\frac{q_{w,i}}{\lambda_w}\left[b_{i+1}E\left(\frac{a}{b_{i+1}}\right) - b_i E\left(\frac{a}{b_i}\right)\right]. \tag{25}$$

Now, employing again the superposition method, it is possible to obtain a solution for any, *a priori* prescribed distribution of $q_w$ which has a circular symmetry. For this purpose, the given heat source should be divided into annular sources of corresponding strength and the resulting temperature distributions should be summed up. We have used this very procedure to calculate $Q_w$. In the wall zone the bubble was divided into annuli so that the liquid layer thickness change in each annulus would not exceed $\pm 5\%$ of the average layer thickness in this annulus. The microlayer thickness was assumed to be approximately constant within each annulus and equal to the average thickness in this annulus.

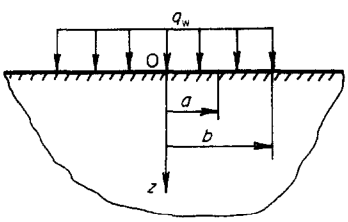


FIG. 3. A semi-infinite body with a circular heat source of radius $b$ [15] attached to the surface.

For the problem to be defined completely, now it remains only to prescribe the minimum dimensionless thickness $\Delta_{min}$. Assume that the minimum microlayer thickness corresponds approximately to intermolecular distances in the liquid, i.e. amounts to $10^{-9}$–$10^{-10}$ m. Then for a bubble of 1 mm in diameter the value of $\Delta_{min}$ will amount to $2\times10^{-6}$–$2\times10^{-7}$. It is for these two values of $\Delta_{min}$ that the problem stated has been solved by the present authors. Running ahead, it should be noted that, as a result, we have obtained two dependencies of $\hat{Q}_w$ on $\xi$. By substituting them into the final relationship for the growth modulus (81), we come to the following conclusion, similar to that of the author of ref. [10], who investigated the growth of bubbles on an isothermal surface: that there is an extremely small influence of the choice of the minimum microlayer thickness on the growth modulus. Thus, a variation of $\Delta_{min}$ by an order of magnitude led to a change of $m$ by no more than 9%. This difference decreases with $\xi$ and when $\xi < 1000$ it does not exceed 1%. Therefore, this has made it possible to ignore the influence of $\Delta_{min}$ on the bubble growth and not to perform calculations for other values of this parameter. For certainty we have chosen the solution with $\Delta_{min} = 2\times10^{-6}$; then the number of annuli turned out to be equal to 132. All the results given below refer to this case.

Before writing a computer program, expressions of the type of equation (25) were nondimensionalized with the aid of equation (16). For example, equation (25) acquired in this case the following form:

$$0 < A < B_i < B_{i+1}$$

$$\Theta_i(\xi, A, 0) = \frac{2}{\pi}\frac{\hat{q}_{w,i}}{\xi}\left[B_{i+1}E\left(\frac{A}{B_{i+1}}\right) - B_i E\left(\frac{A}{B_i}\right)\right]. \tag{26}$$

Calculations were made in the following way. At the beginning of each step, the initial distribution of dimensionless temperature on the wall surface was assigned: $\Theta(\xi, A, 0)$. It was assumed for the first step that $\Theta(\xi, A, 0) = 0$. Then, using equations (18) and (19), the distribution of the dimensionless specific heat flux $\hat{q}_w$ was calculated. Then, using the above-described technique (superposition of calculations from relations of the type of equation (26)), a new distribution, $\Theta(\xi, A, 0)$, was found from the previous one. As the initial distribution for the next step use was made of some intermediate distribution between the new distribution and that one which was initial for the previous step. The calculations were stopped when the newly obtained temperature distribution coincided with the initial one for the given step. In this case, the resulting temperature distribution is such that at each point on the interface the specific heat flux, coming from the wall, is equal to the specific heat flux passing through the microlayer. Thus, boundary condition (18) is fulfilled.

Conditions (20)–(22) are fulfilled automatically because we deal with the superposition of the finite number of Thomas' solutions, for each of which these zero conditions are fulfilled. Therefore, the temperature distribution $\Theta(\xi, A, 0)$ obtained is the solution of the Laplace equation (17) with boundary conditions (18)–(22).

Note that the initial and new distributions of the dimensionless temperature were considered to coincide when the maximum discrepancy between them was less than 0.0001. Our calculations have shown that a further increase of accuracy does not exert any marked effect on the result.

In order to find $\Theta$ on the $z$-axis, we used the analytical solution for a disk source of constant power located on the surface of a semi-infinite body (Fig. 3) [16], which in our notation has the form

$$\theta_i = 2\frac{q_{w,i}\sqrt{(a_w\tau)}}{\lambda_w}\left\{\text{ierfc}\left(\frac{z}{2\sqrt{(a_w\tau)}}\right) - \text{ierfc}\left[\frac{\sqrt{(z^2+b_i^2)}}{2\sqrt{(a_w\tau)}}\right]\right\}. \quad (27)$$

To enable a stationary solution to be found, it is necessary to proceed to the limit $\tau \to \infty$. The change-over to the annular source is realized by the superposition method described above. As a result we obtain the following equation in dimensionless variables for an annular source with radii $B_i$ and $B_{i+1}$:

$$\Theta_i(\xi, 0, Z) = \frac{\hat{q}_{w,i}}{\xi}\left(\sqrt{(Z^2+B_{i+1}^2)} - \sqrt{(Z^2+B_i^2)}\right). \quad (28)$$

Since we already know the values of $\hat{q}_{w,i}$, then, to find $\Theta(\xi, 0, Z)$, it is sufficient to sum up all the results of the calculations from equation (28) for all 132 annuli.

Calculations were made for 20 different values of $\xi$ in the range 20–$10^5$.

The results for some values of $\xi$ are displayed in Table 1. Here, a spherical system of coordinates (Fig. 2) is used. The values of the dimensionless wall temperature $\Theta(\xi, R, \phi)$ are given for two cases: on the liquid boundary, $\Theta(\xi, R, \pi/2)$, and on a straight line which corresponds to the $z$-axis of the Cartesian coordinate system, $\Theta(\xi, R, 0)$. In Fig. 4 the same results at $\phi = \pi/2$ are presented in graphical form. For ease of graphical representation $(T - T_s)/(T_\infty - T_s)$, equal to $(1 - \Theta)$, and not $\Theta$, is plotted along the ordinate. The dimensionless thickness of the liquid microlayer $\Delta$ is also presented.

As is seen from Table 1 and Fig. 4, the wall temperature under a growing bubble can change appreciably only at small values of $\xi$. When $\xi > 10^4$, the wall is heated almost uniformly. Moreover, this conclusion also holds true for non-stationary heat transfer in a wall, since in this case the wall does not succeed in cooling down to a temperature given by the Laplace equation, and therefore it will be still more uniformly heated than in the stationary case. Thus, Labuntsov's assumption [10] that the wall temperature under a growing bubble is constant, holds true at high values of $\xi$. The above relation (14) for a dimensionless heat flux transferred through a liquid microlayer into the bubble is shown in Table 2.

The value of $\hat{Q}_w$ was found by integrating equation (19) over the dimensionless area of the bubble base. For the quantity $\Theta$ we used the obtained distributions of the dimensionless wall surface temperature $\Theta(\xi, R, \pi/2)$. The quantity $\hat{Q}_w$ increases with $\xi$, approaching asymptotically the value of $\hat{Q}_w$ for a uniformly heated wall equal to 76.10.

The above relation for $\hat{Q}_w$ was used to find the bubble growth modulus. For this purpose, we employed the energy balance equation for the bubble in the following form:

$$h\rho_v\frac{dV_b}{d\tau} = Q_w \quad (29)$$

whence we shall obtain for a spherical bubble

$$h\rho_v\frac{d}{d\tau}\left(\frac{4}{3}\pi r_b^3\right) = \hat{Q}_w\lambda_l r_b\theta_s \quad (30)$$

or

$$r_b\,dr_b = \frac{\hat{Q}_w\lambda_l\theta_s}{4\pi h\rho_v}d\tau. \quad (31)$$

Integrating from 0 to $\tau$ yields

$$m = \frac{r_b}{\sqrt{(a_l\tau)}} = \sqrt{\left(\frac{\hat{Q}_w}{2\pi}Ja\right)}. \quad (32)$$

At large values of $\xi$ equation (32) almost coincides with Labuntsov's expression (2) where const. = 12. When $\xi > 10^4$ the values of $m$, calculated from these relations, differ by no more than 1.3%.

Let us evaluate the penetration depth of temperature perturbations in liquid, $l$, using the solution of the problem concerning the cooling of a uniformly heated semi-infinite rod with a constant temperature maintained on its butt-end. The penetration depth can be adopted to be, for instance, such a distance from the butt-end over which the temperature differs by $0.1(T - T_s)$ from the temperature at infinity. Then [16]

$$l \approx 2.32\sqrt{(a_l\tau)} \approx 2\sqrt{(a_l\tau)}. \quad (33)$$

When calculating the quantity $\hat{Q}_w$, we assumed that half of the bubble surface facing downward (Fig. 2) is entirely involved in heat transfer with the wall. However, under certain conditions the height $\delta$ of some part of this surface over the wall can turn to be greater than the temperature disturbance penetration

Table 1. Calculated values of the wall dimensionless temperature under a bubble $\Theta(\xi, R, \phi)$ in the case of quasi-stationary heat transfer

| | $\xi = 20$ | | $\xi = 10^2$ | | $\xi = 10^3$ | | $\xi = 10^4$ | | $\xi = 10^5$ | |
|---|---|---|---|---|---|---|---|---|---|---|
| $R$ | $\phi = \pi/2$ | $\phi = 0$ | $\phi = \pi/2$ | $\phi = 0$ | $\phi = \pi/2$ | $\phi = 0$ | $\phi = \pi/2$ | $\phi = 0$ | $\phi = \pi/2$ | $\phi = 0$ |
| 0.001 | $8.87\times10^{-1}$ | $9.82\times10^{-1}$ | $9.36\times10^{-1}$ | $9.20\times10^{-1}$ | $5.28\times10^{-1}$ | $5.03\times10^{-1}$ | $9.34\times10^{-2}$ | $8.80\times10^{-2}$ | $1.01\times10^{-2}$ | $9.50\times10^{-3}$ |
| 0.01 | 9.90 | 9.06 | 8.78 | 7.14 | 3.59 | 2.75 | 5.56 | 4.29 | $5.91\times10^{-3}$ | 4.56 |
| 0.1 | 7.27 | 5.52 | 3.64 | 2.82 | $7.67\times10^{-2}$ | $6.42\times10^{-2}$ | $9.90\times10^{-3}$ | $8.54\times10^{-3}$ | 1.03 | $8.91\times10^{-4}$ |
| 0.2 | 5.46 | 4.03 | 2.32 | 1.83 | 4.39 | 3.75 | 5.52 | 4.84 | $5.71\times10^{-4}$ | 5.02 |
| 0.3 | 4.36 | 3.21 | 1.72 | 1.37 | 3.11 | 2.68 | 3.86 | 3.42 | 3.99 | 3.54 |
| 0.4 | 3.61 | 2.67 | 1.37 | 1.10 | 2.41 | 2.10 | 2.97 | 2.65 | 3.07 | 2.75 |
| 0.5 | 3.07 | 2.28 | 1.13 | $9.22\times10^{-2}$ | 1.97 | 1.73 | 2.42 | 2.17 | 2.49 | 2.25 |
| 0.6 | 2.64 | 1.99 | $9.61\times10^{-2}$ | 7.93 | 1.66 | 1.47 | 2.03 | 1.84 | 2.09 | 1.90 |
| 0.7 | 2.30 | 1.77 | 8.30 | 6.95 | 1.42 | 1.27 | 1.75 | 1.59 | 1.80 | 1.65 |
| 0.8 | 2.02 | 1.58 | 7.26 | 6.18 | 1.24 | 1.13 | 1.53 | 1.41 | 1.57 | 1.45 |
| 0.9 | 1.78 | 1.44 | 6.40 | 5.56 | 1.10 | 1.01 | 1.35 | 1.26 | 1.39 | 1.30 |
| 1 | 1.55 | 1.31 | 5.65 | 5.06 | $9.78\times10^{-3}$ | $9.13\times10^{-3}$ | 1.20 | 1.14 | 1.24 | 1.17 |
| 2 | $7.22\times10^{-2}$ | $6.95\times10^{-2}$ | 2.69 | 2.63 | 4.75 | 4.68 | $5.87\times10^{-4}$ | $5.79\times10^{-4}$ | $6.06\times10^{-5}$ | $5.98\times10^{-5}$ |
| 3 | 4.78 | 4.69 | 1.79 | 1.77 | 3.16 | 3.13 | 3.90 | 3.88 | 4.03 | 4.01 |
| 4 | 3.57 | 3.54 | 1.34 | 1.33 | 2.36 | 2.36 | 2.92 | 2.92 | 3.02 | 3.01 |
| 5 | 2.85 | 2.84 | 1.07 | 1.06 | 1.89 | 1.89 | 2.34 | 2.33 | 2.41 | 2.41 |
| 6 | 2.38 | 2.37 | $8.91\times10^{-3}$ | $8.88\times10^{-3}$ | 1.58 | 1.57 | 1.95 | 1.95 | 2.01 | 2.01 |
| 7 | 2.04 | 2.03 | 7.63 | 7.62 | 1.35 | 1.35 | 1.67 | 1.67 | 1.72 | 1.72 |
| 8 | 1.78 | 1.78 | 6.68 | 6.67 | 1.18 | 1.18 | 1.46 | 1.46 | 1.51 | 1.51 |
| 9 | 1.53 | 1.58 | 5.93 | 5.93 | 1.05 | 1.05 | 1.30 | 1.30 | 1.34 | 1.34 |
| 10 | 1.42 | 1.42 | 5.34 | 5.34 | $9.45\times10^{-4}$ | $9.45\times10^{-4}$ | 1.17 | 1.17 | 1.21 | 1.21 |

depth $l$ in the liquid. Then this part of the bubble surface will appear to be cut off from heat transfer by the wall. How can this influence the value of $m$?

Let us imagine a plane AA drawn parallel to the wall surface but above this surface by the value $pr_b$ (where $0 < p \leqslant 1$), as shown in Fig. 5. Making use of the previously obtained temperature distribution $\Theta(\xi, R, \pi/2)$ (Table 1), we can assess the heat flux being transferred to that part of the bubble surface which lies beneath the plane AA–$\hat{Q}_p$ and calculate from equation (32) the growth modulus $m_p$, which corresponds to this heat flux. Figure 6 presents the relative deviation

Table 2. Calculated relationship between the dimensionless heat flux $\hat{Q}_w$ and parameter $\xi$

| $\xi$ | $\hat{Q}_w$ | $\xi$ | $\hat{Q}_w$ |
|---|---|---|---|
| $2\times10^1$ | 17.89 | $2\times10^3$ | 65.59 |
| 4 | 24.13 | 4 | 70.04 |
| 6 | 28.15 | 6 | 71.84 |
| 8 | 31.15 | 8 | 72.81 |
| $1\times10^2$ | 33.55 | $1\times10^4$ | 73.42 |
| 2 | 41.30 | 2 | 74.71 |
| 4 | 49.29 | 4 | 75.39 |
| 6 | 53.89 | 6 | 75.62 |
| 8 | 57.04 | 8 | 75.74 |
| $1\times10^3$ | 59.35 | $1\times10^5$ | 75.81 |
| | | $\infty$ | 76.10 |

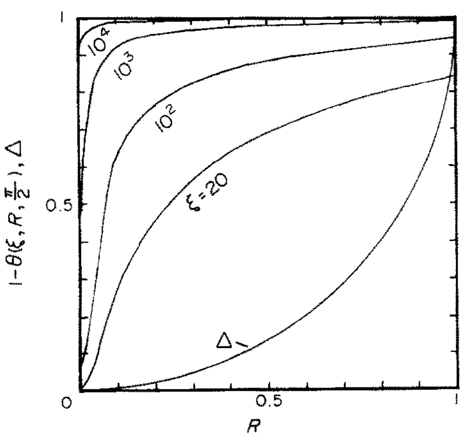


Fig. 4. Dimensionless wall temperature on the boundary with liquid at different $\xi$.

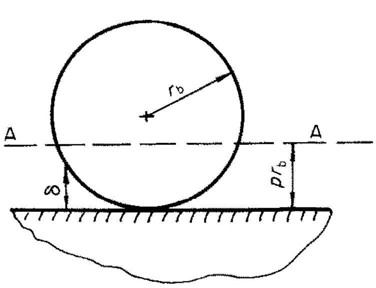


Fig. 5. Diagram of bubble growth at small penetration depths of temperature variations.

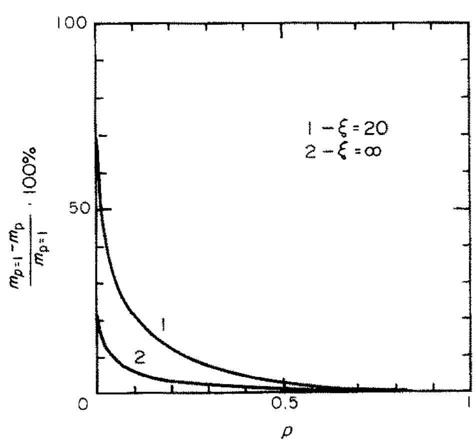


Fig. 6. Relative deviations of the growth modulus on 'cutting out' a part of the bubble surface when $\delta > pr_b$.

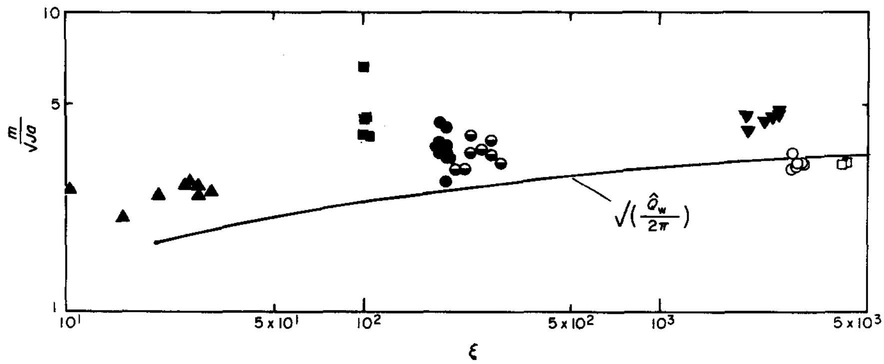


FIG. 7. Comparison of theoretical relation (32) with experimental data. For notation of points see Fig. 11.

$$D = \frac{m_{p=1} - m_p}{m_{p=1}} \quad (34)$$

plotted vs $p$ for two extreme values of $\xi$.

As is evident from this figure, when $p \geqslant 0.4$ the influence of the 'cut-off' part of the surface becomes negligible (the deviation of the growth modulus does not exceed 5%). Therefore, equation (32) can be used when the condition $l \geqslant 0.4 r_b$ is satisfied. With equations (32) and (33) taken into account, this condition can be transformed to

$$m \lesssim 5. \quad (35)$$

Comparison of equation (32), calculated with the use of Table 2, with experimental data, obtained when condition (35) is satisfied, is given in Fig. 7. From this figure it is seen that the theoretical relation agrees qualitatively well with experimental data. However, quantitatively, the majority of experimental points lie slightly above the theoretical curve. This circumstance, which in our opinion is associated with the influence of hèat transfer from superheated liquid layers, is taken into account when the final relationship for the growth modulus is derived in Section 5.

Returning to Table 1, we shall point out an interesting thing: in the case of great radii the temperatures at $\phi = \pi/2$ and 0 are equal. This is not by chance, because, as shown in ref. [17], Thomas' solution for the disk of power $Q_i$ is transformed into the solution for a point source (with double the power, of course, because we deal here with a half-space rather than the entire space):

$$\theta_i = \frac{Q_i}{2\pi r \lambda_w}. \quad (36)$$

Since our solution was obtained by the superposition of $n$ Thomas solutions, then for $r \to \infty$ one can write

$$\theta = \sum_{i=1}^{n} \frac{Q_i}{2\pi r \lambda_w} = \frac{1}{2\pi r \lambda_w} \sum_{i=1}^{n} Q_i \quad (37)$$

or

$$\theta = \frac{Q_w}{2\pi r \lambda_w}. \quad (38)$$

Thus, our solution at infinity should pass to the solution for a point source of the corresponding (double) power. Equation (38) can be written in dimensionless form as

$$\Theta = \frac{\hat{Q}_w}{2\pi R \xi}. \quad (39)$$

With high values of $R$, calculations by equation (39) agree with the data from Table 1 for both $\phi = \pi/2$ and 0. Considerable deviations are observed only at very low $R$.

In the next section we shall need the mean integral wall temperature in the region bounded by a semisphere of radius $R_c$, i.e. $\bar{\Theta}(\xi, R_c)$. As is shown in Appendix A, this value can be calculated approximately using relation (39) from the following equation:

$$\bar{\Theta}(\xi, R_c) = \frac{3\hat{Q}_w}{4\pi \xi R_c} \quad (40)$$

which is valid when $R_c^2 \gg 0.09$.

## 4. THE RANGE OF APPLICABILITY OF THE QUASI-STATIONARY MODEL

We shall try to determine conditions under which heat transfer in a heating wall follows the stationary law. Divide the heating wall under the bubble by a semisphere of radius $r_0$, with the centre coinciding with the centre of the bubble base, into two parts: region I with $0 \leqslant r \leqslant r_0$ and region II with $r_0 \leqslant r$ (Fig. 8). Determine the maximum dimensionless tempera-

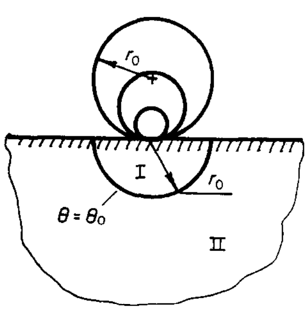


FIG. 8. Determination of the limits of the quasi-stationary approach applicability.

ture on the boundary of regions I and II, i.e. $\Theta_0^{max}$ which is achieved on bubble growth.

When $c_w\rho_w$ is high, the heat accumulated in the wall will hinder its cooling during bubble growth. Therefore, we shall assume that the wall will be cooled the most when $c_w\rho_w \to 0$, i.e. when the quasi-stationary approximation is valid (see Section 2). Then, $\Theta_0$ can be calculated, with some overestimation, by relation (40) which can be rewritten in the form

$$\Theta_0 = \frac{\hat{Q}_w}{2\pi\xi}\frac{r_b}{r_0}. \tag{41}$$

This quantity takes its largest value when $r_b = r_0$

$$\Theta_0^{max} = \frac{\hat{Q}_w}{2\pi\xi}. \tag{42}$$

Calculations from this relation with the use of Table 2 showed that in the considered range of $\xi$ the value of $\Theta_0^{max}$ does not exceed 0.14. This means that no less than 86% of the total temperature difference is realized in region I and in the microlayer, that is, essential in this case will be the thermal processes that proceed only in these regions, whereas the thermal resistance of region II can be neglected. (The accuracy of this approximation can be improved by taking a somewhat greater radius for zone I, but this is of no principal importance for further analysis.)

Thus, to determine the region of the quasi-stationary approximation applicability, it is necessary to find the conditions under which the heat capacity of region I cannot exert an appreciable effect on heat transfer to the bubble. We will assume that these conditions are satisfied in the case when the maximum possible variation of the internal energy of region I for the time of bubble growth $\Delta E_I$ is much smaller than the heat transferred to the bubble from the wall during that time, $E_w$:

$$\frac{\Delta E_I}{E_w} \ll 1. \tag{43}$$

As already pointed out, the existence of heat capacity $c_w\rho_w$ should prevent the wall cooling and, consequently, the decrease of the temperature difference in the microlayer. Therefore, we will assume that $E_w$ will reach its minimum value when $c_w\rho_w \to 0$ (with other conditions being equal). This means that to find $E_w^{min}$, we can make use of the quasi-stationary approximation

$$E_w^{min} = \int_0^{\tau_0} Q_w \, d\tau \tag{44}$$

where $Q_w$ is found with the help of Table 2.

Since

$$\frac{\Delta E_I}{E_w^{min}} \geqslant \frac{\Delta E_I}{E_w} \tag{45}$$

then to satisfy condition (43), it is sufficient that

$$\frac{\Delta E_I}{E_w^{min}} \ll 1. \tag{46}$$

A great number of experiments demonstrate that the bubble growth curves $r_b = f(\tau)$ are rather well approximated by the relations of the type

$$r_b = M \cdot \tau^n \tag{47}$$

where $M$ and $n$ are constants if the characteristic dimension of the heater is close to or exceeds the bubble departure diameter. We consider here only low and moderate $Ja$ (Section 6). In this case the value of $n$ is close, as a rule, to 0.5 and for the overwhelming majority of data it lies within the range 0.3–0.7.

Therefore, we shall assume that

$$n = 0.5 \pm 0.2. \tag{48}$$

From equation (47) it follows that

$$r_b = r_0\left(\frac{\tau}{\tau_0}\right)^n. \tag{49}$$

Then, equation (44) will yield

$$E_w^{min} = \int_0^{\tau_0} \hat{Q}_w \lambda_l \theta_s r_0 \left(\frac{\tau}{\tau_0}\right)^n d\tau \tag{50}$$

i.e.

$$E_w^{min} = \frac{1}{n+1}\hat{Q}_w \lambda_l \theta_s r_0 \tau_0. \tag{51}$$

In accordance with equation (48), the value of $1/(n+1)$ is equal to 0.68 accurate to 13%, therefore we can write

$$E_w^{min} \approx 0.68 \hat{Q}_w \lambda_l \theta_s r_0 \tau_0. \tag{52}$$

The maximum value of $\Delta E_I$ can be readily evaluated as

$$\Delta E_I = \frac{2}{3}\pi r_0^3 c_w \rho_w \theta_s. \tag{53}$$

But this evaluation is much overestimated because it implies that for the period of the bubble growth the temperature at all the points of region I will change from $T_\infty$ to $T_s$. However, as it was pointed out above, the maximum cooling, with all other conditions being equal, takes place when $c_w\rho_w \to 0$. Then the minimum mean integral temperature of region I can be approximately calculated from relation (40) and the maximum temperature can be taken as $T_\infty$. Then we can obtain

$$\Delta E_I = \frac{2}{3}\pi r_0^3 c_w \rho_w \frac{3\hat{Q}_w}{4\pi\xi(r_0/r_b)}\theta_s. \tag{54}$$

This value will reach its maximum when $r_b = r_0$ ($R_c = 1$)

$$\Delta E_I^{max} = \frac{\hat{Q}_w}{2\xi} r_0^3 c_w \rho_w \theta_s. \tag{55}$$

Then, to satisfy inequality (46) and, consequently, condition (43), it is sufficient that

$$\frac{(\hat{Q}_w/2\xi)r_0^3 c_w \rho_w \theta_s}{0.68\hat{Q}_w \lambda_l \theta_s r_0 \tau_0} \ll 1 \quad (56)$$

whence

$$a_w \tau_0 / r_0^2 \gg 0.7$$

i.e.

$$Fo \gg 0.7. \quad (57)$$

This condition has a clear physical meaning. Indeed, the quantity $r_0^2/a_w$ can be interpreted as the scale of the relaxation time of thermal disturbances [12]. Then, in accordance with inequality (57), for the process to be quasi-stationary (i.e. in order that the system could pass successively through an infinite number of its stationary states, each of which corresponds to the microlayer configuration available at the given moment), it is necessary that the characteristic time for the process $\tau_0$ be much in excess of the relaxation time $r_0^2/a_w$.

Usually, the bubble growth rate is characterized by the growth modulus

$$m = \frac{r_b}{\sqrt{(a_l \tau)}}. \quad (58)$$

The determination of this quantity from the departure parameters $(\tau_0, r_0)$ will yield

$$Fo = \frac{a_w/a_l}{m^2}. \quad (59)$$

It will be shown in Section 5 that the accurate calculation of heat influx from the wall to the bubble is meaningful only at small $Ja$ ($\lesssim 13$), and this, by the way, is true for the greater portion of the practically important range in boiling of liquids. Experiments show that in this case $m \lesssim 10$ and it decreases with $Ja$. Since in the majority of cases the ratio $a_w/a_l$ lies in the range $10^2$–$10^6$, the quasi-stationary heat transfer model in the heating wall can be expected to have quite a wide range of applicability. We shall return to this problem in Section 6 when comparing the theoretical relation for the growth modulus with experimental data.

## 5. BUBBLE GROWTH MODULUS

We will assume that the bubble surface can be divided into three parts. The first part, the surface area of which is equal to $S_w$, is supplied with heat from the wall $Q_w$ through an adjacent liquid 'microlayer'; the second part (the surface area is $S_l$) is supplied with heat $Q_l$ from the surrounding superheated liquid; the third part which, in our opinion, can exist at sufficiently large $Ja$, is not supplied with heat at all.

We will assume that the heat flux from the heating wall can be transferred only to those points on the lower part of the bubble surface the height of which above the wall $\delta$ (Fig. 2) is smaller than the penetration depth of the temperature perturbation into liquid $l$ (33). Then, when $l > r_b$, or, equivalently

$$m \lesssim 2 \quad (60)$$

it can be assumed that heat is transferred from the wall to the entire downward facing bubble surface through a 'microlayer'. Thus, for the case considered the value of $S_w$ is equal to $2\pi r_b^2$, and the heat flux from the wall can be found from Table 2. To condition (60) there correspond small numbers of $Ja$ ($\lesssim 0.5$). At such small values of $Ja$ the bubble departure diameters are usually lower than $10^{-3}$ m [7, 18–20]. On the other hand, direct measurements [21, 22] show that the thickness $\delta_T$ of the superheated liquid layer formed on the wall in nucleate boiling is of the order of $10^{-4}$ m, i.e. it is comparable with the bubble size. Therefore, it is logical to suppose for the case considered that the bubble is completely covered with a superheated liquid layer, a part of which is pushed away from the wall during the process of growth (Fig. 9(a)). Then $S_l = 2\pi r_b^2$.

When the bubble grows far beyond the superheated layer, which is observed, for instance, in nitrogen and oxygen boiling when $Ja \gtrsim 10$–$20$ [23–25], it is probable that the superheated layer thickness in the upper part of the spherical surface will decrease greatly. Then one can ignore this part of the superheated layer in thermal calculations. We shall suppose for this case that when growing the bubble pushes aside and away from the wall a part of the superheated layer to be accumulated under the downward facing half of the bubble surface (Fig. 9(b)), i.e. the area covered with the superheated liquid constitutes $2\pi r_b^2$. This value can be refined when comparing the thus derived relationship for the bubble growth modulus with experimental data.

To calculate heat inflow from the superheated liquid, it is necessary to solve the system of equations that describe the motion and heat transfer in the superheated liquid layer on a portion of the bubble surface with corresponding initial and boundary conditions and with the conditions of conjugation at the phase interface. To simplify calculations, we shall assume that only the radial velocity exists in the liquid surrounding the growing bubble (here and hereafter the spherical coordinate system will be used the centre of which coincides with the bubble centre) and that temperature and velocity fields in the superheated liquid layer depend only on $r$ and $\tau$. Then the energy conservation equation in this layer can be expressed as

$$\frac{\partial \theta}{\partial \tau} + U\frac{\partial \theta}{\partial r} = \frac{a_l}{r^2}\frac{\partial}{\partial r}\left(r^2 \frac{\partial \theta}{\partial r}\right). \quad (61)$$

We shall ignore inertia forces which may be appreciable only at high $Ja$. Also neglected will be the mass forces, which, as shown experimentally [22], do not

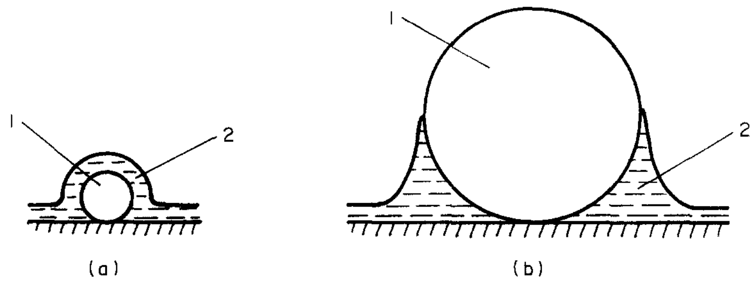


FIG. 9. Bubble growth at small (a) and high (b) Jakob numbers: 1, vapour bubble; 2, superheated liquid layer.

influence the growth modulus and also the viscosity and surface tension forces.

Under the above conditions the Navier–Stokes equation will reduce to

$$p = \text{const.} \tag{62}$$

which will also be valid for the vapour phase.

The continuity equation will have the form

$$\frac{1}{r^2}\frac{\mathrm{d}}{\mathrm{d}r}(r^2 U) = 0. \tag{63}$$

The initial conditions will be stated as

$$\tau = 0, \quad r_b = 0 \tag{64}$$

$$\tau = 0, \quad \theta = 0. \tag{65}$$

Now, we can write down the boundary conditions. As was mentioned before, the superheated liquid layer thickness $\delta_T$ has the order of $10^{-4}$ m. Of the same order is the depth of temperature perturbation penetration into liquid $l$, calculated from equation (33), for the bubble growth time equal to 0.01–1 s. This allows us to suppose that the thermal processes near the bubble surface will follow the same course as in the case of $\delta_T = \infty$.

Then, the condition at infinity can be formally expressed as

$$r \to \infty, \quad \theta \to 0. \tag{66}$$

Neglecting the thermal resistance on the liquid–vapour interface and taking into account equation (62), we can express the condition on the inner boundary of the bubble in the form

$$r = r_b, \quad \theta = \theta_s. \tag{67}$$

The analysis of Scriven's tabulated data [1] demonstrated that if one restricts oneself to the region of

$$\frac{h}{c_l(T_\infty - T_s)} > 10 \tag{68}$$

which is of greatest practical interest, then to determine the growth modulus it is possible to use, with a sufficient accuracy, the solution with the parameter $(\rho_l - \rho_v)/\rho_l = 1$ [3]. Virtually this means that for the compatibility condition for the mass fluxes the liquid–vapour interface can be assumed impermeable. In this case the above-mentioned condition can be given in the form

$$U_b = \frac{\mathrm{d}r_b}{\mathrm{d}\tau} \tag{69}$$

which will be used in what follows.

The compatibility condition for energy fluxes will be written as

$$\frac{\mathrm{d}}{\mathrm{d}\tau}(V_b h \rho_v) = Q_l + Q_w \tag{70}$$

where

$$Q_l = \lambda_l \left.\frac{\partial \theta}{\partial r}\right|_{r=r_b} \cdot S_l. \tag{71}$$

We shall now consider separately the above-indicated cases of small and large $Ja$.

### 5.1. *Small Ja*

As already mentioned, in this case the value of $Q_w$ can be calculated from

$$Q_w = \hat{Q}_w \lambda_l \theta_s r_b \tag{72}$$

where $\hat{Q}_w$ is determined from Table 2.

To find the bubble growth law, it is necessary to solve the system of equations (61)–(63) with initial conditions (64), (65), boundary conditions (66), (67) and the compatibility conditions (69)–(72). The analysis of this system shows that the problem is fully described by the following set of variables: $r, \tau, \theta_s, a_l, h\rho_v, \lambda_l, \hat{Q}_w$, the last one being dimensionless, that is

$$\theta = f_3(r, \tau, \theta_s, a_l, h\rho_v, \lambda_l, \hat{Q}_w) \tag{73}$$

and

$$r_b = f_4(\tau, \theta_s, a_l, h\rho_v, \lambda_l, \hat{Q}_w). \tag{74}$$

Using the dimensional analysis, the latter expression can be transformed into

$$m = \frac{r_b}{\sqrt{(a_l \tau)}} = f_4(Ja, \hat{Q}_w). \tag{75}$$

It is shown in Appendix B that the solution of the problem set can be presented in the form of the following equation:

$$1 = \left(\frac{m^2}{Ja} - \frac{\hat{Q}_w}{2\pi}\right)\int_1^\infty \frac{1}{R^2}\exp\left[-\frac{m^2}{2}\left(\frac{1-R}{R} + \frac{R^2-1}{2}\right)\right]dR \quad (76)$$

which establishes equation (75) in an implicit form. The definite integral in equation (76) is not expressed, in the general case, in terms of elementary functions. It was calculated by Scriven numerically [1]. We will denote it by $F(m)$. The values of this function, obtained by recalculation from Scriven's solution, are given in Table 3. It has two asymptotes

$$m \ll 1, \quad F(m) \to 1 \quad (77)$$

$$m \gg 1, \quad F(m) \to \sqrt{\left(\frac{\pi}{3}\right)}\Big/ m. \quad (78)$$

Equation (76) can be approximated accurate to about 4% by

$$m = \left[\left(\sqrt{\left(\frac{3}{\pi}\right)} Ja\right)^{3/2} + \left(\sqrt{\left(\left(\frac{\hat{Q}_w}{2\pi}+1\right)Ja\right)}\right)^{3/2}\right]^{2/3}. \quad (79)$$

(When $m \ll 1$ and $m \gg 1$ the agreement is perfect.) Taking into account the approximate nature of this approach, it is possible to omit the coefficient $\sqrt{(3/\pi)}$, equal to 0.98, and to use the expression

$$\gamma = \left(\frac{\hat{Q}_w}{2\pi}+1\right)^{3/4} \approx \frac{6.9}{(1+1070/\xi)^{0.23}} \quad (80)$$

instead of determining $\hat{Q}_w$.

Table 3. Function $F(m)$ obtained by means of recalculation from Scriven's solution [1] at $(\rho_l - \rho_v)/\rho_l = 1$

| $m$ | $F(m)$ |
|---|---|
| 0.02 | 0.98250 |
| 0.04 | 0.96575 |
| 0.08 | 0.93344 |
| 0.12 | 0.90333 |
| 0.16 | 0.87500 |
| 0.2 | 0.84850 |
| 0.4 | 0.73513 |
| 0.8 | 0.57812 |
| 1.2 | 0.47500 |
| 1.6 | 0.40250 |
| 2 | 0.34885 |
| 4 | 0.20850 |
| 8 | 0.11509 |
| 12 | 0.07943 |
| 16 | 0.06063 |
| 20 | 0.04902 |
| 40 | 0.02504 |
| 80 | 0.01265 |
| 120 | 0.00847 |
| 160 | 0.00636 |
| 200 | 0.00509 |
| 400 | 0.00255 |
| 600 | 0.00170 |
| 800 | 0.00128 |

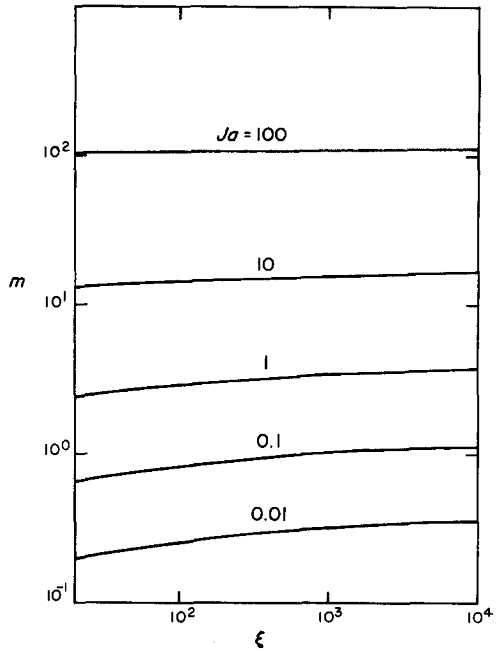


FIG. 10. The influence of solid wall relative thermal conductivity on the vapour bubble growth modulus at different Jakob numbers.

The error of the growth modulus calculation due to the use of the above relation does not exceed 1.3%. Hence, we shall finally obtain

$$m = (Ja^{3/2} + \gamma Ja^{3/4})^{2/3} \quad (81)$$

where $\gamma$ is found from relation (80).

5.2. *Large Ja*

In this case the heat transfer from the wall will involve a considerably smaller portion of the bubble surface (for which $\delta \lessapprox l$). However, it is in this region that the most intensive heat transfer from the wall is concentrated, as is evident from Fig. 6. Therefore, in this case too the value of $\hat{Q}_w$, though with lesser accuracy, can be found from Table 2. But since in this case the bubble growth will be mainly controlled by the heat inflow from the liquid, there is no sense in the accurate determination of $\hat{Q}_w$, as it will be shown later.

The surface area of the bubble covered with superheated liquid has been already determined as equal to $2\pi r_b^2$. Then, when assuming again that in the vicinity of this surface the same assumptions hold for the temperature and velocity fields as in Section 5.1, it will be necessary to solve the same system of equations (61)–(63) with the same boundary conditions. Naturally, the solution will remain the same too.

Thus we have come to the conclusion that in both the region of small $Ja$ and the region of high $Ja$ the solution is specified by the same function. Therefore, one can expect this function to describe the process at any values of $Ja$. Comparison with experimental data in Section 6 confirms this hypothesis. Thus, for fluids under consideration, regardless of the value of $Ja$, it is possible to recommend relation (81) for calculating the growth modulus.

Figure 10 presents a schematic diagram of the relation obtained. As is seen, the dependence of the growth modulus on $\xi$ becomes increasingly weaker with the growth of *Ja*. It is due to the fact that as *Ja* increases, the role of the second term in the parentheses on the right-hand side of equation (81), which accounts for heat transfer from the wall, becomes smaller. Beginning from $Ja \approx 13$, the main part is played, according to equation (81), by heat transfer from superheated liquid, $Q_l$, irrespective of the values of $\xi$.

### 6. COMPARISON WITH EXPERIMENT

We compared relation (81) with experimental data of seven works containing the results of a cinematographic investigation into the boiling of cryoagents (helium, hydrogen, nitrogen, oxygen), freons (F-12, F-113, F-142), ethanol and benzene on surfaces that differ considerably in thermal properties (copper, silver, stainless steel, nickel, German silver, constantan). Experimental conditions are summarized briefly in Table 4 which shows that the values of $\xi$, responsible for heat transfer from the wall in the quasi-stationary mechanism of heat transfer, varied within a wide range from 10 to 4220.

The range of *Ja* was also broad enough: from 0.4 to 83. Moreover, we compared calculations by relation (81) with experimental data on ethanol boiling when $Ja > 100$ [27–29]. It appeared that in this region equation (81) slightly overpredicts experimental data probably due to inertial effects. Therefore, the resulting relation is recommended to be used when $Ja \leqslant 100$.

Two works are worthy of special attention. When processing the data of ref. [19] we had to use the following relation:

$$m = \frac{r_0}{\sqrt{(a_l \tau_0)}} \tag{82}$$

with $\tau_0$ including not only the time of growth, but also the silence time of nucleation sites. It is shown in ref. [19] that at the lowest pressures the fraction of the silence time increased and in separate cases it could be approximately equal to the growth time. Therefore, the data on boiling in vacuum from the above-mentioned work were not used by us.

The authors of ref. [24] studied the growth of bubbles on the upper generatrix of a horizontal tube where, as they claim, there seem to exist upstream flows of superheated liquid. It is to this effect that these authors attribute the extraordinary behaviour of bubbles after their departure: they continued their growth at the same rate as on the heater, with the post-departure growth time being sometimes several fold higher than the pre-departure growth time [25]. It might be for this reason that at high *Ja* the results of that work can be described by the Plesset–Zwick formula for pool boiling which was obtained on the assumption that the entire bubble surface was covered with superheated liquid. As far as equation (81) is concerned, it underpredicts the values of *m* from ref. [24] by 30–50%.

Figure 11 compares experimental data from all the papers except ref. [24] with the final equation (81). From this figure it can be seen that experimental results are satisfactorily described by this relation. For the majority of points the difference between theoretical and experimental values of the growth modulus does not exceed $\pm 35\%$.

In Section 4 an approximate condition of the applicability of the quasi-stationary model (57) was obtained. Now, we can attempt to refine it by comparing experimental data with theoretical results at different *Fo*. However, the data of all the papers except ref. [24] are in a satisfactory agreement with the final relation (81) in spite of a wide range of *Fo*. But, there is no essential mystery about it. As it has been already

Table 4. Experimental conditions

| Ordinal No. 1 | Authors 2 | Fluid 3 | Surface 4 | *Fo* (relation (59)) 5 | $\xi$ 6 | *Ja* 7 |
|---|---|---|---|---|---|---|
| 1 | Grigoriev *et al.* [2] | Nitrogen | Copper | 3.7 | 1600 | 7.47 |
| 2 | | | Nickel | 0.81–2.8 | 360 | 4.01–11.4 |
| 3 | | | Stainless steel | 0.26 | 74 | 15.3 |
| 4 | Pavlov and Potekhin [7] | Helium | Copper | $1.1 \times 10^5$–$3.8 \times 10^5$ | 1900–2500 | 0.4–1.79 |
| 5 | | | Stainless steel | 12–83 | 10–31 | 1.6–6.5 |
| 6 | Kirichenko and Levchenko [18] | Hydrogen | German silver | 1.3–3.7 | 100–113 | 0.68–34.7 |
| 7 | Gladchenko [23] | Oxygen | Constantan | 0.055–45 | 144–192 | 0.47–83 |
| 8 | Kirichenko *et al.* [24, 25] | Nitrogen | Stainless steel | 0.071–0.40 | 51–63 | 4.1–10 |
| 9 | | Oxygen | | $4.4 \times 10^{-3}$–5.6 | 47–89 | 0.3–89 |
| 10 | Danilova [19] | Freon 12 | Stainless steel | 1.0–25 | 170–290 | 0.39–6.3 |
| 11 | | Freon 113 | | 1.0 | 260 | 18.6 |
| 12 | | Freon 142 | | 0.55 | 160 | 10.2 |
| 13 | Grigoriev *et al.* [2] | Ethanol | Copper | 3.1–4.8 | 2590 | 8.19–13.5 |
| 14 | | | Nickel | 0.35 | 556 | 22.0 |
| 15 | | | Stainless steel | 0.20 | 98.0 | 14.2 |
| 16 | Golovin *et al.* [26] | Ethanol | Silver | 24–2500 | 2710–3000 | 0.115–9.54 |
| 17 | | Benzene | | 4.8–191 | 3310–4220 | 1.5–33.8 |

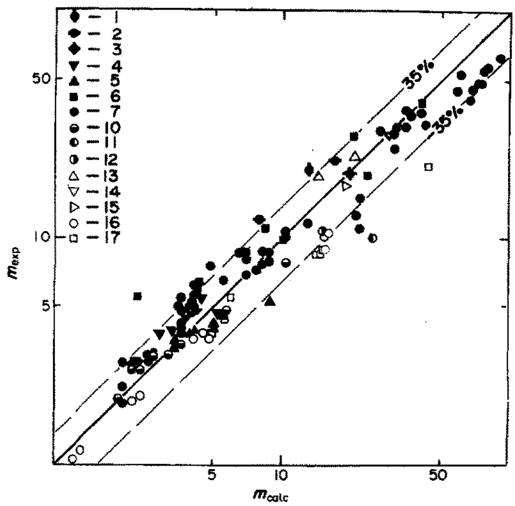

FIG. 11. Comparison of final equation (81) with experimental data on the vapour bubble growth rate. The numbering of points correspond to Table 4.

pointed out, the ratio $a_w/a_l$ usually varies within the range $10^2$–$10^6$. Therefore, $Fo$ substantially smaller than 0.7 may be observed only at high values of $m$ (large $Ja$). But, as shown in Section 5, in this case the heat transfer through a microlayer, $Q_w$, for the bubble growth is small and decreases with an increase of $m$. Therefore, in spite of the fact that the quasi-stationary approximation becomes invalid for $Fo \ll 0.7$, equation (81) can be formally used in this case too. Thus, the now available experimental data do not justify any constraint on the use of equation (81) with respect to $Fo$, with the only restriction being the condition $Ja \lesssim 100$ beyond which the energy scheme of the vapour bubble growth ceases to operate. The above condition does not impose serious restrictions on the generality of equation (81), because it is violated only at very low reduced pressures ($p/p_{cr} < 0.005$). Thus, there are good reasons to suppose that the influence of the thermal properties of the heating surface material on the bubble growth rate, and, consequently, on boiling heat transfer can be described by a single solid body parameter, i.e. its thermal conductivity, instead of the set of properties $(\rho c\lambda)_w$ in the nucleate boiling non-stationary model [2, 7, 11]. It is also possible to suppose the existence of a whole class of phenomena in which the space–time nonuniformity of the heat transfer coefficient (heat transfer in turbulent flow, natural convection, condensation, boiling) is accompanied by quasi-stationary heat conduction in the wall and the value of the average heat transfer coefficient will depend on $\xi$. This conclusion is to a certain degree confirmed by the results of refs. [30, 31], where a satisfactory correlation of heat transfer data for both boiling and vaporization of liquids in forced channel flow was achieved with the help of $\xi$.

## 7. CONCLUSIONS

(1) Vapour bubble growth for the case of small wetting angles was considered. It is shown that heat transfer in the heating wall under a growing bubble can be realized quasi-stationarily, i.e. so that the temperature distributions in the heater do not considerably differ from stationary ones. The condition is established to approximately determine the region of the applicability of this approach.

(2) In order to calculate the quasi-stationary heat transfer from the wall to a spherical bubble, $Q_w$, the Laplace equation was solved for the temperature field in the wall. Furthermore, with heat transfer from superheated liquid $Q_l$ being taken into account, an equation is obtained for the vapour bubble growth modulus, i.e. equation (81), without empirical coefficients. This equation quite satisfactorily predicts experimental data for liquids that can easily wet the heating surface. This correlation is applicable when $\xi \gtrsim 10$ and $Ja \lesssim 100$.

(3) The effect of thermal properties of the heater material on the vapour bubble growth and, consequently, on boiling heat transfer rate can be taken into account by the simplex $\lambda_w/\lambda_l$, which characterizes the quasi-stationary heat transfer in the heating wall. There are reasons to suppose that this conclusion will hold true for a wide class of problems which are characterized by the space–time nonuniformity of the heat transfer coefficient.

## REFERENCES


1. L. E. Scriven, On the dynamics of phase growth, *Chem. Engng Sci.* **10**(1), 1–14 (1959).
2. V. A. Grigoriev, Yu. M. Pavlov and Ye. V. Ametistov, *Boiling of Cryogenic Fluids.* Izd. Energia, Moscow (1977).
3. D. A. Labuntsov and V. V. Yagov, *Mechanics of Simple Gas–Liquid Structures.* Izd. MEI, Moscow (1978).
4. D. A. Labuntsov, Up-to-date ideas on the mechanism of nucleate boiling of liquids. In *Heat Transfer and Physical Gas Dynamics.* Izd. Nauka, Moscow (1974).
5. P. J. Marto, J. A. Moulson and M. D. Maynard, Nucleate pool boiling of nitrogen with different surface conditions, *J. Heat Transfer* **90**(4), 437–444 (1968).
6. D. Steinbrecht, Einfluss der Wärmeleitzahl des Heizflachenmaterials auf die Wärmeübergangszahlen beim Blasensieden, *Wiss. Z. TH Magdeb.* **14**(8), 929–930 (1970).
7. Yu. M. Pavlov and S. A. Potekhin, Bubble growth rate during boiling in the region of moderate and high pressures, *Trans. Moscow Pwr Engng Inst.* No. 478, 43–54 (1980).
8. V. Magrini and E. Nannei, On the influence of the thickness and thermal properties of heater on the heat transfer coefficients in nucleate pool boiling, *J. Heat Transfer* **97**(2), 173–178 (1975).
9. A. S. Dudkevich and F. D. Akhmedov, Experimental investigation of the effect of thermal properties of the heater on nitrogen boiling at elevated pressures, *Trans. Moscow Pwr Engng Inst.* No. 198, 41–47 (1974).
10. D. A. Labuntsov, Mechanism of vapour bubble growth in boiling on the heating surface, *J. Engng Phys.* **6**(4), 33–39 (1963).
11. M. G. Cooper and R. M. Vijuk, Bubble growth in nucleate pool boiling, *Proc. 4th Int. Heat Transfer Conf.*, Paris, Vol. 5, paper B 2.1 (1970).

12. S. S. Kutateladze, *Similarity Analysis and Physical Models*. Izd. Nauka, Novosibirsk (1986).
13. Shih-Pin Liaw and V. K. Dhir, Effect of surface wettability on transition boiling heat transfer from a vertical surface, *Proc. 8th Int. Heat Transfer Conf.*, San Francisco, Vol. 4, pp. 2031–2036 (1986).
14. S. Shakir and J. R. Thome, Boiling nucleation of mixture on smooth and enhanced surfaces, *Proc. 8th Int. Heat Transfer Conf.*, San Francisco, Vol. 4, pp. 2081–2086 (1986).
15. P. H. Thomas, Some conduction problems in the heating of small areas on large solids, *Q. J. Mech. Appl. Math.* **10**(4), 482–493 (1957).
16. H. S. Carslaw and J. C. Jaeger, *Conduction of Heat in Solids*, 2nd Edn. Oxford University Press, London (1959).
17. J. V. Beck, Large time solution for temperature in a semi-infinite body with a disk heat source, *Int. J. Heat Mass Transfer* **24**, 155–164 (1981).
18. Yu. A. Kirichenko and N. M. Levchenko, Investigation of internal characteristics of boiling hydrogen, *Zh. Prikl. Mekh. Tekh. Fiz.* No. 4, 103–108 (1976).
19. G. N. Danilova, Heat transfer of boiling freons, D.Sc. Thesis, Leningrad Technological Institute of Refrigeration Industry, Leningrad (1968).
20. V. S. Golovin, Experimental investigation of heat transfer, crisis and mechanism of boiling organic fluids under conditions of natural convection, Ph.D. Thesis, Energy Institute, Moscow (1967).
21. T. E. Lippert and R. S. Dougall, A study of the temperature profiles measured in the thermal sublayer of water, Freon-113 and methyl alcohol during pool boiling, *J. Heat Transfer* **90**(3), 347–352 (1968).
22. B. D. Marcus and D. Dropkin, Measured temperature profiles within the superheated boundary layer above a horizontal surface in saturated nucleate pool boiling of water, *J. Heat Transfer* **87**(3), 333–341 (1965).
23. G. M. Gladchenko, Nucleate boiling of oxygen in low body-force fields under different pressures, Ph.D. Thesis, Physico-Technical Institute for Low Temperatures, Kharkov (1986).
24. Yu. A. Kirichenko, V. V. Tsibulski, M. L. Dolgoy, K. V. Rusanov and I. M. Konoval, Effect of pressure on internal characteristics of boiling nitrogen and oxygen, *J. Engng Phys.* **28**(4), 581–588 (1975).
25. Yu. A. Kirichenko, V. V. Tsibulski, M. L. Dolgoy, K. V. Rusanov and I. M. Konoval, Cinematographic investigation of nitrogen and oxygen boiling process. In *Problems of Hydrodynamics and Heat Transfer in Cryogenic System*, No. 3, pp. 56–63. Physico-Technical Institute for Low Temperatures, Kharkov (1973).
26. V. S. Golovin, B. A. Kolchugin and E. A. Zakharova, Measurement of vapour bubble growth rate in boiling of various fluids, *Teplofiz. Vysok. Temp.* **4**(1), 147–148 (1966).
27. V. V. Yagov, Investigation of boiling liquids (mechanism, heat transfer, augmentation) in the region of low pressures, Ph.D. Thesis, Moscow Power Engineering Institute, Moscow (1971).
28. A. K. Gorodov, O. N. Kaban'kov, A. T. Komov, Yu. K. Martynov and V. V. Yagov, Experimental investigation of vapour bubble dynamics in water and ethanol boiling in the region of low pressures, *Trans. Moscow Pwr Engng Inst.* No. 268, 33–42 (1975).
29. M. Akijama, F. Tachibana and N. Ogawa, Effect of pressure on bubble growth in pool boiling, *Bull. J.S.M.E.* **12**(53), 1121–1128 (1969).
30. V. V. Klimenko and A. V. Grigoriev, An approximate theory of nucleate flow boiling in tubes, *Izv. AN SSSR, Energet. i Transp.* No. 6, 116–125 (1983).
31. V. V. Klimenko, Boiling heat transfer in forced channel flow, *Heat Transfer—Sov. Res.* **17**(2), 96–100 (1985).

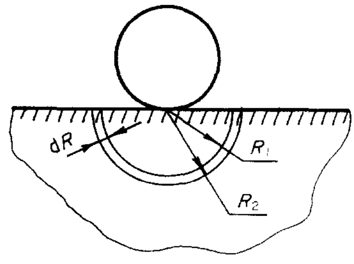


FIG. A1. Spherical layer in the d$R$-thick wall.

## APPENDIX A. CALCULATION OF THE MEAN INTEGRAL WALL TEMPERATURE $\bar{\Theta}(\xi, R_c)$ IN THE REGION $R \leqslant R_c$

Let $\bar{\Theta}_*(\xi, R)$ be the mean temperature of a hemispherical layer of thickness d$R$ and radius $R = (R_1+R_2)/2$ (Fig. A1). It is evident that the mean integral temperature of a hemispherical region can be calculated as

$$\bar{\Theta}(\xi, R_c) = \frac{3/2}{\pi R_c^3}\int_0^{R_c} \bar{\Theta}_*(\xi, R)\,\mathrm{d}\left(\frac{2}{3}\pi R^3\right). \quad \text{(A1)}$$

In accordance with the solution obtained earlier for large $R$'s, $\Theta$ on the ray $\phi = 0$ coincides with $\Theta$ on the ray $\phi = \pi/2$ and with function (39). It is obvious that in this case the temperature of the layer at all the points is the same and the mean temperature of the layer can be found from relation (39).

As the radius decreases, $\Theta$ on the ray $\phi = \pi/2$ begins to exceed $\Theta$ on the ray $\phi = 0$. The mean temperature of the layer in this case is to satisfy the inequality

$$\Theta(\xi, R, 0) < \bar{\Theta}_*(\xi, R) < \Theta(\xi, R, \pi/2). \quad \text{(A2)}$$

Since function (39) gives an intermediate result between $\Theta(\xi, R, 0)$ and $\Theta(\xi, R, \pi/2)$, we shall use it to estimate $\bar{\Theta}_*(\xi, R)$ for this case too. However, when $R < 0.3$, it gives an overprediction.

How much will it affect the value of $\bar{\Theta}(\xi, R_c)$? To answer this question, we shall find $\bar{\Theta}(\xi, R_c)$ from equation (A1) using relation (39) and first having divided the region of integration into two parts: 0–0.3 and 0.3–$R_c$. We shall obtain

$$\bar{\Theta}(\xi, R_c) = \frac{3\hat{Q}_w}{4\pi\xi R_c^3}[(0.3^2-0)+(R_c^2-0.3^2)]. \quad \text{(A3)}$$

It is obvious that when the condition $R_c^2 \gg 0.09$ is observed, it is possible to ignore the first term in square brackets which characterizes the temperature in the region 0–0.3, despite the fact that relation (39) was used which overpredicts the results in this very region. It means that in the case considered the inaccuracy of relation (39) will not considerably influence the value of the mean integral temperature of the region 0–$R_c$ which can be calculated from relation (40).

## APPENDIX B. SOLUTION OF THE SYSTEM OF EQUATIONS (61)–(63)

As is seen from equation (75), the quantities $\tau$ and $r_b$ are related unambiguously for the given conditions. Therefore, it is possible to replace $\tau$ by $r_b$ in equation (73). This will give

$$\Theta = \hat{f}_3(R, Ja, \hat{Q}_w). \quad \text{(B1)}$$

Since the last two quantities in the function term do not vary during the process of growth, one can assume for the given solutions that

$$\Theta = \Theta(R). \quad \text{(B2)}$$

Then, using the rules of complex function differentiation one can obtain the following relations for the derivatives of equation (61):

$$\frac{\partial \theta}{\partial \tau} = \theta_s \frac{d\Theta}{dR}\frac{\partial R}{\partial r_b}\frac{dr_b}{d\tau} = -\theta_s \frac{d\Theta}{dR}\frac{R}{r_b}\frac{dr_b}{d\tau} \tag{B3}$$

$$\frac{\partial \theta}{\partial r} = \theta_s \frac{d\Theta}{dR}\frac{\partial R}{\partial r} = \theta_s \frac{d\Theta}{dR}\frac{1}{r_b}. \tag{B4}$$

To calculate $U$ it is possible to use the continuity equation (63), from which it follows that

$$r^2 U = \text{const.} = r_b^2 U_b. \tag{B5}$$

Then

$$U = U_b\left(\frac{r_b}{r}\right)^2 = \frac{U_b}{R^2}. \tag{B6}$$

Using these expressions and equation (69), the energy conservation equation (61) can be reduced to the form

$$\left(\frac{r_b\, dr_b/d\tau}{a_l}\right)\left(\frac{1-R}{R^2}\right)\frac{d\Theta}{dR} = \frac{1}{R^2}\frac{d}{dR}\left(R^2\frac{d\Theta}{dR}\right). \tag{B7}$$

Using equation (75), it is possible to show that the first expression in parentheses on the left-hand side of equation (B7) does not depend on time and is equal to $m^2/2$. Thus, we shall obtain the following equation from equations (61), (63), and (69):

$$\frac{m^2}{2}(R^{-2}-R)\frac{d\Theta}{dR} = \frac{1}{R^2}\frac{d}{dR}\left(R^2\frac{d\Theta}{dR}\right). \tag{B8}$$

The initial condition is fulfilled automatically, because we use relation (75). The second initial condition, equation (65), in dimensionless form will yield

$$R = \infty, \quad \Theta = 0. \tag{B9}$$

This condition is also a dimensionless form of boundary condition (66). The second boundary condition, equation (67), which also includes the equation of motion (62), results in the expressions

$$R = 1, \quad \Theta = 1. \tag{B10}$$

Combining relations (70)–(72), we shall obtain the following expression in dimensionless form:

$$\left.\frac{d\Theta}{dR}\right|_{R=1} = \frac{m^2}{Ja} - \frac{\hat{Q}_w}{2\pi}. \tag{B11}$$

The integration of equation (B8) is carried out in the same way as in ref. [3]. First consider the quantity $R^2\, d\Theta/dR$ as a new variable. Then the first integration of the above equation will give

$$R^2\frac{d\Theta}{dR} = \text{const.} \exp\left[-\frac{m^2}{2}\left(\frac{1}{R}+\frac{R^2}{2}\right)\right]. \tag{B12}$$

To determine the constant of integration, we shall use condition (B11)

$$\frac{d\Theta}{dR} = \left(\frac{m^2}{Ja} - \frac{\hat{Q}_w}{2\pi}\right)\frac{1}{R^2}\exp\left[-\frac{m^2}{2}\left(\frac{1-R}{R}+\frac{R^2-1}{2}\right)\right]. \tag{B13}$$

The integration of the last expression within the range from $R = 1$ to $R$ will yield the temperature field

$$1-\Theta = \left(\frac{m^2}{Ja} - \frac{\hat{Q}_w}{2\pi}\right)\int_1^R \frac{1}{R^2}\exp\left[-\frac{m^2}{2}\left(\frac{1-R}{R} + \frac{R^2-1}{2}\right)\right] dR. \tag{B14}$$

This relation satisfies condition (B10). Condition (B9) leads to equation (76).

## CROISSANCE DE BULLE DE VAPEUR DANS L'EBULLITION AVEC DES CONDITIONS QUASI-STATIONNAIRES DE TRANSFERT THERMIQUE DANS LA PAROI CHAUFFANTE

**Résumé**—On étudie la croissance des bulles de vapeur dans l'ébullition sur une paroi solide avec des petits angles de mouillage. On constate que le transfert de chaleur dans la paroi sous la bulle peut se faire dans un mode quasi-stationnaire. Les limites de l'applicabilité de cette approche ont été déterminées. La solution de l'équation de Laplace $\nabla^2 T = 0$ décrit le champ de température dans le cas considéré. On obtient une formule théorique pour le module de croissance de bulle de vapeur sans aucune constante empirique. Cette formule prédit convenablement les données expérimentales pour les liquides cryogéniques, Freons et autres, qui mouillent facilement une surface solide. Il est établi que l'effet du matériau du chauffoir peut être pris en compte à l'aide d'un paramètre simple, la conductivité relative $\lambda_w/\lambda_l$.

## DAMPFBLASENWACHSTUM BEIM SIEDEN UNTER QUASI-STATIONÄREN WÄRMEÜBERTRAGUNGSBEDINGUNGEN AN EINER BEHEIZTEN WAND

**Zusammenfassung**—Es wurde das Wachstum der Dampfblasen beim Sieden an einer festen Wand mit kleinem Benetzungswinkel untersucht. Es wird gezeigt, daß die Wärmeübertragung in der Wand unter der Blase in einer quasi-stationären Weise ablaufen kann. Die Grenzen der Anwendbarkeit dieser Näherungsbetrachtungen wurden bestimmt. Die Lösung für die Laplace-Gleichung $\nabla^2 T = 0$ wird gegeben, welche das Temperaturfeld für den betrachteten Fall beschreibt. Man erhält eine theoretische Beziehung ohne empirische Konstanten für das Dampfblasenwachstum. Die Beziehung gibt experimentelle Daten für Kältemittel und andere Flüssigkeiten, die eine Heizfläche gut benetzen, zufriedenstellend wieder. Es wurde festgestellt, daß der Einfluß des Heizflächenmaterials mit Hilfe eines einfachen Parameters—der relativen Wärmeleitfähigkeit—erklärt werden kann.

## ЗАКОНОМЕРНОСТИ РОСТА ПАРОВЫХ ПУЗЫРЕЙ ПРИ КИПЕНИИ В УСЛОВИЯХ КВАЗИСТАЦИОНАРНОГО ТЕПЛООБМЕНА В ГРЕЮЩЕЙ СТЕНКЕ

**Аннотация**—Рассмотрен рост паровых пузырей на твердой стенке для случая малых углов смачивания. Показано, что теплообмен в стенке под основанием пузыря может осуществляться квазистационарно, определены границы применимости данного подхода. Получено решение уравнения Лапласа $\nabla^2 T = 0$, описывающего поле температур для этого слчая. С учетом теплоподвода из стенки и из перегретой жидкости получено теоретическое соотношение для модуля роста парового пузыря при кипении, не содержащее ни одного эмпирического коэффициента. Это соотношение вполне удовлетворительно описывает экспериментальные данные для криогенов, фреонов и других жидкостей, хорошо смачивающих поверхность нагрева. Установлено, что влияние материала поверхности нагрева может быть учтено с помощью параметра относительной теплопроводности $\lambda_w/\lambda_l$.